

Conformational chain statistics in a model lipid bilayer: Comparison between mean field and Monte Carlo calculations

Daniel Harries and Avinoam Ben-Shaul

*Department of Physical Chemistry and The Fritz Haber Research Center,
The Hebrew University of Jerusalem, Jerusalem 91904, Israel*

(Received 9 August 1996; accepted 16 October 1996)

A comparison between a mean field theory of chain packing in membranes and micelles and Monte Carlo simulations is presented for model lipid bilayers. In both approaches the "lipids" are modeled as freely jointed (but self-avoiding) chains of spherical segments. The first segment of the chain represents the head group, anchored to the bilayer interface by a harmonic binding potential. The simulations are performed for symmetric bilayers composed of 200 chains, with periodic boundary conditions. Both pure and mixed bilayers (composed of long and short chains) are analyzed. In the simulation nonbonded segments interact via Lennard-Jones potentials, ensuring nearly uniform segment density in the bilayer core, as assumed in the mean field theory. The lateral pressure profiles governing the probability distribution of chain conformations in the mean field theory are related and compared to the tangential pressure profiles calculated from the simulations using Kirkwood–Buff's molecular theory. The two pressure profiles show very good agreement. We also calculate two conformational chain properties: end-segment distributions and orientational bond order parameters. The end-segment distributions calculated by the two approaches show excellent agreement. The order parameters compare somewhat less satisfactorily, yet we found that the order parameters derived from the simulations depend rather sensitively on the details of the interaction potential. In general, the results of the simulations support the use of the mean field theory as a (simple) tool for studying conformational chain statistics in confined environments and related thermodynamic properties, such as membrane curvature elasticity. © 1997 American Institute of Physics. [S0021-9606(97)50604-0]

I. INTRODUCTION

A number of molecular mean field theories have been proposed in the last two decades or so, in order to explain the molecular organization and conformational statistics of lipid bilayers.^{1–6} Related theories have been proposed for polymer brushes.^{7,8} The proliferation of these approximate theories reflects the difficulty of studying these complex, many-molecule, systems by large scale computer simulations. Although the number of accurate simulation studies (especially molecular dynamics, MD, simulations) is growing steadily, they are still limited to a few specific systems under selected conditions. Apart from some of the inherent difficulties associated with computer simulations, such as uncertainties in the intermolecular potentials used and the limited time scales followed, there are certain phenomena which cannot be studied by these approaches, at least not in the foreseeable future. Among those are, for instance, slow spontaneous (long wavelength) curvature fluctuations of lipid membranes, or the process of protein incorporation into a lipid bilayer. Thus, although computer simulation studies will obviously further develop and contribute to the understanding of membrane structure, dynamics and thermodynamics, it is also clear that approximate, partly analytical, theories will continue to play an important role in analyzing these systems, especially in predicting and explaining general trends and qualitative behaviors.

Some of the mean field (MF) theories have been tested, generally with considerable success, by comparing their pre-

dictions to experimental results and simulation studies.^{1,2(b),6,7} These comparisons involve, usually, measurable conformational chain properties such as orientational bond order parameters and spatial distributions of the hydrophobic tail segments. However, most comparative studies between mean field theories and computer simulations, are limited to few special cases, and are based on similar but not identical molecular models.

Our goal in this paper is to compare the predictions of one, widely applied, mean field theory¹ of lipid in membranes with Monte Carlo (MC) computer simulations for the same molecular model, and for a wide range of conditions. Since our primary objective is to compare these two computational schemes, we have chosen a very simple model for the "lipid" molecules constituting the bilayer. We treat them as flexible linear chains, consisting of n identical spherical segments ("beads"), connected by bonds of fixed length. Nearest neighbor beads can rotate (wiggle) freely with respect to each other, except for excluded volume interactions between nonbonded segments. The first chain segment, representing the polar head group is anchored to the membrane interface by a strong harmonic binding potential. Ideally we should have modeled the chains, as in the MF calculations, as chains of hard spheres. However, unlike in hard sphere fluids, achieving uniform density in a bilayer composed of such chains is only possible at very high (nearly close packing) segment densities. At such densities the system is essentially frozen ("glassy") and it is impossible to reach true

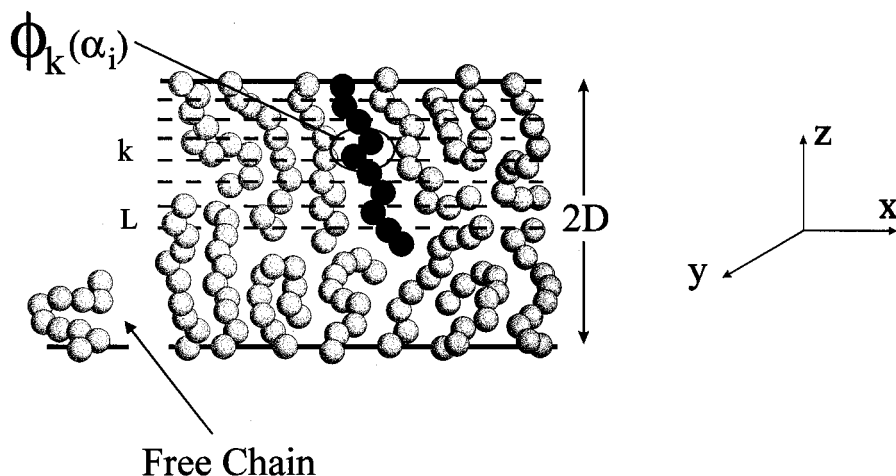


FIG. 1. Schematic illustration of a membrane bilayer, of thickness $2D$, parted into $2L$ sublayers. The quantity $\phi_k(\alpha_i)$ denotes the number of segments of a chain in conformation α_i whose centers fall within sublayer k . The conformations of chains in the bilayer are generally more elongated as compared with a free (non-interacting) chain.

dynamical equilibrium. Thus in the MC simulations of the bilayer, we have replaced the hard sphere interactions between nonbonded segments by 6-12 Lennard-Jones potentials. The attractive parts of these potentials should provide the uniform attractive background and the short range repulsive interactions should govern the chain packing statistics, i.e., the molecular conformations. For comparative purposes we have also performed simulations using “sticky-ball” interaction potentials between nonbonded segments, i.e., hard core repulsion and r^{-6} attraction.

It should be emphasized that in the MF calculations the interaction potential appears only indirectly, through the assumption of uniform chain segment density in the hydrophobic core of the membrane. It also should be noted that while in the simulations nonbonded chain segments, including those belonging to the same chain, interact via Lennard-Jones potentials we do not include these interactions in the MF theory. The reason for this apparent difference, is that in the simulated system the attractive potentials (between all kinds of nonbonded segments), are necessary to achieve uniform monomer density. On the other hand, in the MF theory uniform monomer density is assumed at the outset, and there is no justification to distinguish between different kinds of nonbonded interactions.

In Sec. II we briefly outline the MF theory and in Sec. III we describe the bilayer and chain models, as well as the MC simulation algorithm. Sec. IV is devoted to a discussion of the lateral pressure profile appearing in the MF expression for the probability distribution of chain conformations. In the MC simulations we calculate the tangential pressures using the molecular theories of Kirkwood–Buff^{9–11} and Harasima.¹⁰ In Sec. IV we elaborate on the relationship between the two types of pressure profiles. In Sec. V we compare the results obtained by these two approaches for pure (single component) bilayers as well as for mixed bilayers composed of both short and long chains.

II. MEAN FIELD THEORY

The theory outlined in this section and its applications to such issues as membrane curvature elasticity, monolayers, and lipid-protein interaction have been described in considerable detail elsewhere.^{1,4–6} Therefore, in this section we shall only mention the essential assumptions and expressions relevant for the derivation of our expression for the probability distribution of chain conformations. In Sec. IV we shall elaborate on the significance of the lateral pressures which appear in the MF calculations and, in a somewhat different form, in the MC calculations.

The only assumption underlying the mean field theory is the existence of a well defined hydrophobic region, uniformly packed by chain segments. The segment density may be identified with that of a bulk liquid hydrocarbon composed of the lipid tails. Subject to this assumption one can derive an explicit expression for the probability distribution of chain conformation $P(\alpha)$, for a hydrophobic core of arbitrary geometry. (In fact, one need not assume a uniform density throughout the hydrophobic core. It is sufficient to know the density profile.) Among these geometries are those of spherical and cylindrical micelles, inverted (e.g., cubic) lipid phases and vesicles of any curvature. Here, however, we shall only be concerned with planar bilayers, as schematically depicted in Fig. 1.

Consider a planar and symmetric bilayer of (hydrophobic) thickness $2D$ and a total area A (at each interface). Thus the membrane volume is $V=2AD$. For computational purposes it is convenient to divide the volume of the hydrophobic core into $2L$ parallel sublayers, each of thickness λ . Let $M_k=\lambda A_k$ denote the volume of sublayer k , with A_k denoting its total area. In the planar bilayer $M_k=M$ and $A_k=A$ are constant; later on it will prove useful to treat M_k and A_k as variables. Suppose there are N chains (head groups) anchored to each of the two bilayer interfaces. Thus the av-

erage area per head group in the bilayer is $a=A/N$. The average volume per chain is $V/2N=aD=v$. If the bilayer is composed of n -segment chains then $v=n\nu$ where ν is the average volume per segment.

We shall use $\alpha_1, \dots, \alpha_N, \bar{\alpha}_{N+1}, \dots, \bar{\alpha}_{2N} \equiv \alpha^N \bar{\alpha}^N$ to denote a particular, many-chain, configuration of the membrane, with α_i denoting the conformation of chain i , originating at one of the two bilayer interfaces, and $\bar{\alpha}_j$ denoting the conformation of chain j originating from the opposite interface. Note that chains originating from opposite interfaces can inter-digitate, i.e., they can cross the bilayer midplane.

Let $\phi_k(\alpha_i)$ denote the number of segments of chain i which, when this chain is in conformation α_i , (the centers of which) fall within sublayer k of the bilayer. Since the segment density in the hydrophobic core is uniform, we must have

$$\sum_{i=1}^N \phi_k(\alpha_i) + \sum_{j=1}^N \phi_k(\bar{\alpha}_j) = M_k/\nu \quad (1)$$

for all the possible many-chain configurations $\alpha^N \bar{\alpha}^N$.

Let

$$P(\alpha) = \sum_{\alpha_2, \dots, \alpha_N} \sum_{\bar{\alpha}_1, \dots, \bar{\alpha}_N} \mathbf{P}(\alpha_1, \dots, \bar{\alpha}_{2N}) \quad (2)$$

denote the probability of finding chain 1 in conformation $\alpha_1 = \alpha$, with $\mathbf{P}(\alpha_1, \dots, \bar{\alpha}_{2N})$ denoting the probability of the many chain configuration. Since all chains are equivalent $P(\alpha_i)$ is the same (singlet) probability distribution for all chains (i or j). Now, multiplying Eq. (1) by Eq. (2) and summing over all $\alpha^N, \bar{\alpha}^N$, we find

$$\begin{aligned} \langle \psi_k \rangle &= \langle \phi_k \rangle + \langle \bar{\phi}_k \rangle = \sum_{\alpha} P(\alpha) \phi_k(\alpha) + \sum_{\bar{\alpha}} P(\bar{\alpha}) \phi_k(\bar{\alpha}) \\ &= \sum_{\alpha} P(\alpha) [\phi_k(\alpha) + \phi_{2L-k+1}(\alpha)] \\ &= m_k/\nu \quad (\text{all } k), \end{aligned} \quad (3)$$

where $m_k = M_k/N = a_k \lambda$, with $a_k = A_k/N$. In passing to the second equality we have used the symmetry properties $P(\alpha) = P(\bar{\alpha})$ and $\phi_k(\bar{\alpha}) = \phi_{2L-k+1}(\alpha)$ with α and $\bar{\alpha}$ denoting mirror image conformations (i.e., $\bar{\alpha}$ is the same chain conformation as α except that the chain originates from the opposite interface).

Equation (3), expressing the condition of uniform segment density, represents a set of packing constraints (one for each sublayer k) on the singlet probability distribution $P(\alpha)$. Note that only $2L-1$ of these constraints are independent, since $\sum_k \langle \psi_k \rangle = 2n$ where n is the number of chain segments. In a symmetric planar bilayer the number of independent constraints is only $L-1$ since $\langle \psi_k \rangle = \langle \psi_{2L-k+1} \rangle$.

Among the many $P(\alpha)$ which satisfy (3), the ‘‘true’’ distribution is the one which minimizes the free energy functional $F(\{P(\alpha)\})$ subject to the packing constraints (3). Explicitly, the conformational Helmholtz free energy, in the mean field approximation, is given by

$$\begin{aligned} F/N &= \sum_{\alpha} P(\alpha) [\epsilon(\alpha) + kT \ln P(\alpha)] \\ &+ \sum_{\bar{\alpha}} P(\bar{\alpha}) [\epsilon(\bar{\alpha}) + kT \ln P(\bar{\alpha})], \end{aligned} \quad (4)$$

where, again, the two terms on the right account for the free energies, per molecule, of chains originating from opposite interfaces. (For a symmetric, single component, bilayer these two contributions must be equal.) In the last equation $\epsilon(\alpha)$ is the internal energy of a chain in conformation α (e.g., *trans/gauche* energy in the case of alkyl chains), k is Boltzmann’s constant and T the absolute temperature. In the model considered in this study we set $\epsilon(\alpha) \equiv 0$ and hence the free energy involves only the entropic contribution, $F = -TS$.

Minimization of Eq. (4) subject to Eq. (3) yields

$$P(\alpha) = \frac{1}{q} \exp \left[-\beta \epsilon(\alpha) - \beta \sum_{k=1}^{2L} \pi_k \phi_k(\alpha) \right] \quad (5)$$

with the (isothermal-isobaric) partition function q ensuring the normalization of $P(\alpha)$. The π_k ’s are the Lagrange multipliers conjugate to the packing constraints (3); π_k can be interpreted as the lateral (or tangential) pressure acting in sublayer k on a given chain by its neighbors. In a hypothetical bilayer composed of non-interacting (free, or ‘‘ghost’’) chains all the π_k ’s vanish identically and hence $P(\alpha)$ is a simple canonical distribution. If in addition all $\epsilon(\alpha) = 0$ then $P(\alpha) = 1/\Omega$, i.e., the distribution is microcanonical with all allowed conformations being equally probable.

In a real membrane the chains are squeezed by their neighbors and are thus stretched along the membrane normal, resulting in non-zero lateral pressures. The smaller the cross-sectional area per chain in the membrane, the larger are the π_k ’s. The π_k ’s are generally large near the interfaces and decrease towards the bilayer midplane; reflecting the fact that the average shape of a free chain is that of a ‘‘turnip’’—wide near the interface and narrowing down towards the bilayer midplane. Since the ϕ_k ’s are dimensionless the π_k ’s have the dimensions of energy. Thus π_k/ν has the dimensions of energy/volume and can be interpreted as an ‘‘ordinary’’ tangential pressure. Similarly, $\pi_k(\lambda/\nu)$ can be interpreted as the lateral pressure (energy/area) in layer k . We shall elaborate on these interpretations in Sec. IV.

The numerical values of the π_k ’s are determined by substituting Eq. (5) back into the packing constraints (3), thus obtaining a set of $2L$, self-consistency equations which can be solved numerically for the π_k ’s. In a symmetric bilayer we must have $\pi_k = \pi_{2L-k+1}$. Note also that since (for all α) $\sum_k \phi_k(\alpha) = n$, the number of chain segments, one can add an arbitrary constant c to all the π_k ’s without affecting $P(\alpha)$; [since the sum $\sum_k \pi_k \phi_k(\alpha)$ appears also in q]. Thus as noted above, the number of independent equations that need to be solved is $L-1$ rather than $2L$. [In general the lowest π_k corresponds to the bilayer midplane, $k=L$ or $L-1$ in Fig. 1. In fact, it can be shown that in adsorbed (Langmuir) monolayers all π_k ’s are non-negative; the lateral pressure vanishes towards the chain end.¹] The numerical solution of the self-consistency equations involves the generation and

enumeration of a very large number of chain conformations (typically many millions), from which one determines the $\{\phi_k(\alpha)\}$ required for the evaluation of the π_k 's.

It should be emphasized that while the uniform density assumption underlies the packing constraints (3), the actual density does not enter our calculations. Equation (3) only states that $\langle \phi_k \rangle = n/L = n(\lambda/D) = \text{constant}$, i.e., the average number of segments is the same at any distance from the interface. Thus the π_k 's depend on the chain length n and membrane thickness D . Assuming that the hydrophobic core is liquid-like we can infer the average area per head group from $a = (n\nu)/D$ where ν is the average segment volume in the bulk liquid hydrocarbon. Note, however, that neither a nor ν are required for calculating the π_k 's.

Once $P(\alpha)$ is known, we can calculate any desired conformational (single) chain property, such as bond orientational order parameters and spatial distributions of different chain segments. Similarly, using Eq. (4) one can calculate the free energy per chain and related thermodynamic properties (such as curvature elasticity⁵). In this paper, however, we shall focus on conformational properties. Calculations of such properties for pure ($n=10$ segment long chains) and mixed ($n=10, m=5$) systems will be described in Sec. V.

Finally, it should be mentioned that the probability distribution function, $P(\alpha)$ of Eq. (5), which was derived here by minimizing the mean field free energy subject to the relevant packing constraints, can also be derived on the basis of a more general statistical thermodynamic approach.^{1,5} In this approach one starts from the many-chain partition function, corresponding to a particular conformation α of one "central" chain, and expands this partition function in powers of the $\phi_k(\alpha)$'s. Equation (5) is then obtained in the limit $N \gg 1$. The assumption underlying this derivation is that the conformational statistics of the chains are dominated by the repulsive (excluded volume) interactions between (nonbonded) segments belonging to different chains. The long range van der Waals forces only provide a uniform attractive background, ensuring uniform segment density throughout the hydrophobic core.

III. MODEL

In all our simulations and mean field calculations, for both pure (single component) and mixed systems, the bilayer is planar and symmetric, i.e., containing the same number of chains in each monolayer. In the case of a pure bilayer N chains originate from each of the two ("hydrocarbon-water") interfaces. The lipids are modeled as single chains of n identical segments, with the first segment representing the polar head group, Fig. 2. The head group is anchored to the interface by a harmonic potential, allowing small displacements of the chain along the membrane normal. (We have also performed calculations for a square-well binding potential, the results being similar.) The distance between successive segments, i.e. the bond length σ , is fixed. We use the bond length $\sigma=1$ as our length unit. There are no restrictions on inter-bond angles, except for those arising from ex-

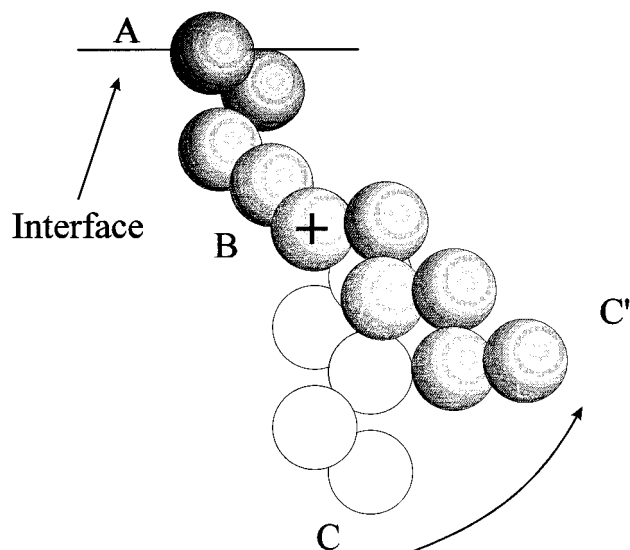


FIG. 2. Illustration of the modified Pivot-algorithm used in the Monte Carlo simulations. A chain segment (B) is selected at random to serve as a pivot point. Then an attempt is made to rotate the whole part of the chain emanating at that point by a small angle ($BC \rightarrow BC'$). This trial move is accepted or rejected according to the Metropolis scheme.

cluded volume interactions between nonbonded chain segments. These restrictions are slightly different for the MF and MC simulations, as detailed below.

A. Mean field calculations

In the mean field calculations the lipid molecule is modeled as a chain of hard spheres of diameter σ . All (non-intersecting) chain conformations are allowed, provided no segment (center) protrudes beyond the bilayer boundaries. Subject to this restriction and, of course, to chain connectivity, every segment (sphere) can pivot freely around its neighbors. A large number of chain conformations (typically between 1 and 2 million) are generated as follows: We randomly choose one of the first $n-1$ chain segments (i.e., excluding the terminal segment). Suppose this is segment i . We then attempt a small random rotation (by $\pi/22$) of the rest of the chain (segments $i+1, \dots, n$) around this segment. The new conformation is accepted provided there is no violation of excluded volume or boundary restrictions. In addition to bond rotations (chain pivoting or wiggling), we also allow the head group to oscillate within the harmonic restoring well, accepting or rejecting the move according to the standard (Metropolis) MC procedure. This is a modification of the Pivot (or wiggling) algorithm used in some simulations of polymeric systems.¹⁴⁻¹⁷

For every conformation sampled we calculate the segment distribution $\{\phi_k(\alpha)\}$ which is then used in the self-consistency equations for the π_k 's. Note that we sample all the allowed chain conformations with equal probabilities. However, their actual statistical weight is governed by $P(\alpha)$ which, in turn, depends on the π_k 's. Qualitatively, the smaller the cross sectional area per chain a (larger D), the larger the lateral pressures and, as expected, stretched out

chain conformations are more probable than expanded conformations.

B. MC simulations

In the MF calculations we *assume* that the segment density is uniform throughout the hydrophobic core. We thus require that the uniform density condition is also satisfied in the simulated system. Note, however, that in the MC simulations the segment density is an outcome of the lateral chain packing density ($1/a$) and the intermolecular forces between (nonbonded) chain segments. Thus uniform density is not automatically satisfied and must be checked.

In all the MC simulations we have modeled bilayers of 200 chains, $N=100$ chains originating at each interface. The distance, $2D$, between the two interfaces was adjusted in order to achieve uniform segment density in the hydrophobic core. The same value of D was used in the MF calculations. Periodic boundary conditions in the xy (bilayer) plane ensure the integrity of the membrane.

The parameters used for the Lennard-Jones potential $u(r)=4\epsilon[(\sigma/r)^{12}-(\sigma/r)^6]$ were $\sigma=1$ (i.e., equal to the bond length between chain segments) and $\epsilon/k=88$ K. The head groups are bound to the interface by a harmonic potential, with a force constant $\kappa/k=768$ K/ σ^2 . This corresponds to an oscillation amplitude of $\langle z_1^2 \rangle^{1/2}=(kT/\kappa)^{1/2}\cong 0.67\sigma$. The value of ϵ in the Lennard-Jones potential between chain segments corresponds to the depth of the potential well between CH_2 segments in liquid hydrocarbons.¹⁵ In general, a nearly uniform monomer density in the bilayer was achieved at a volume fraction $\rho\cong 0.44$ (~ 0.6 of the close-packing density). The value of $\rho\cong 0.44$ corresponds to $\rho\sigma^3\cong 0.84$ which is typical for liquid-like densities.

Beginning with some arbitrary allowed chain configuration, simulation steps were carried out according to the same pivoting (wiggling) procedure described for the MF calculations. In the MC simulations we have also allowed for head group displacement within the xy plane, thus mimicking lateral diffusion of the chains. Flip-flop movements were not allowed. Starting at a very high temperature (3×10^6 K) the system was cooled down slowly to 350 K, a temperature still higher than the expected temperature of the liquid-crystalline–gel transition. The system was “aged” until the potential energy fluctuations stabilized at about 0.02 kT /chain with constant values for configurational averages. We assume that at this stage the system has reached equilibrium. At equilibrium we have sampled conformational properties over long periods of MC time, only for the innermost 36 chains in the simulation box. Samples were taken every 25 MC steps. In most calculations at least 5 sets, each consisting of about 1000 samples were taken.

C. Conformational properties

To compare between the MF and MC calculations we have chosen two common conformational properties, directly derived from $P(\alpha)$: The spatial distribution (along the membrane normal) of the terminal chain segment, and the bond orientational order parameter profile of the chains. We have

also compared the lateral (tangential) pressure profiles in the membrane, as obtained by the two approaches. This comparison involves certain assumptions, as will be discussed in Sec. IV.

(I) End segment distribution.

Let $z_i(\alpha)$ denote the normal distance of the i th segment of some (arbitrarily chosen) chain in conformation α originating, say, at the lower bilayer interface from the bilayer midplane (Fig. 1); ($i=1$ denotes the head group and $i=n$ the end segment). Then $z'_i(\alpha)=z_i(\alpha)-z_1(\alpha)$ is the normal distance of the i th segment from the head group. Since $z_1(\alpha)$ is confined to a very narrow range around z_1 , $P(\alpha)$ is essentially independent of $z_1(\alpha)$. We define $Q_n(z')$ as the end group distribution, i.e., $Q_n(z')dz'$ is the probability of finding the end segment within the interval $z', z'+dz'$. Formally

$$Q_n(z')=\sum_{\alpha} P(\alpha)\delta(z'-z'_n(\alpha)) \quad (6)$$

with $\delta(x)$ denoting Dirac's delta function. In practice we calculate $Q_n(z')$ by dividing the core into sublayers $z_k, z_k+\lambda$ (Fig. 1) and monitoring the frequency of observing the end segment in the k 's sublayer.

(II) Orientational order parameters

Let $\theta_k(\alpha)$ denote the angle between the membrane normal and the vector connecting segments $k-1$ and $k+1$ of a chain in conformation α . We define the (skeletal) orientational order parameters by

$$S_k=\sum_{\alpha} P(\alpha)P_2(\cos\theta_k(\alpha))=\langle P_2(\cos\theta_k) \rangle, \quad (7)$$

where $P_2(x)=(3x^2-1)/2$ is the second Legendre polynomial. For a fully stretched (“all-*trans*”) chain parallel to the membrane normal $S_k\equiv 1$ for all k , whereas for a random distribution of bond orientations $S_k\equiv 0$. Note that in a membrane, due to the existence of an impenetrable interface, the S_k 's are not necessarily zero even in the absence of inter-chain interactions.

IV. LATERAL PRESSURE PROFILES

The lateral pressure profile $\{\pi_k\}$, or $\pi(z)$ if we use a continuous representation, uniquely determines our mean field conformational distribution $P(\alpha)$, and hence all the conformational and thermodynamic properties derived from this function. It would be interesting to compare the π_k 's with a corresponding function which might be derived from the MC simulations. The natural choice of this quantity is the tangential pressure profile $p_T(z)$, familiar from the theory of phase boundaries and surface tension.¹¹ Thus in the next section, we present numerical results and comparisons of the π_k 's with $p_T(z)$, the latter calculated using the molecular theories of Kirkwood–Buff⁹ and Harasima¹⁰ (KBH). The comparison of the two quantities is, however, not entirely straightforward because: (a) the MF and MC models are not strictly identical, and (b) the membrane interface, at least in our calculations, is not a simple phase boundary, namely, it is sharply defined and in principle tensionless. To clarify

these statements we shall now briefly reiterate the relevant forces acting in a lipid membrane and their relationship to the lateral and tangential pressure profiles.

Suppose we change, at constant T , the membrane area from A to $A+dA$, keeping its total volume $V=2DA$ constant, so that $dD=-(D/A)dA$. By definition, the work done on the system in this process is $dW=2\Gamma dA$, where Γ is the effective surface tension of the membrane and the factor 2 accounting for the fact that the bilayer has two interfaces. (We use the term ‘‘effective’’ for Γ to distinguish it from the hydrocarbon-water surface tension.) This work can also be expressed as $dW=dF-2Ap_N dD=dF+2(1/D)p_N dA$ with dF denoting the change in the internal free energy of the membrane (including the interaction potential between surface chain segments and the aqueous solvent), and p_N is the external pressure acting normal to the membrane interfaces. Since V and T are constant it follows that $F=F(A)$ and hence $dF=(\partial F/\partial A)_{v,T} dA=2(\partial f/\partial a)_{v,T} dA$ with $f=F/2N$ and $a=A/N$ denoting, respectively, the free energy and the average head group area per molecule in the membrane. Thus

$$\Gamma = \left(\frac{\partial f}{\partial a} \right)_v + Dp_N, \quad (8)$$

where it should be noted that, formally, this equation refers to one of the two identical membrane monolayers.

The free energy per molecule, f , involves several contributions. One of those, the conformational free energy, f_c (which in our MF model is fully entropic) has been discussed in Sec. II. Additional contributions arise from inter-head group repulsions, chain-chain attractions and chain-water (‘‘hydrophobic’’) interactions. In our model the head groups are simply the first chain segments and hence their interactions are included in f_c , which already accounts (albeit indirectly) for chain-chain repulsions.

From our assumption that the chain segments in the hydrophobic region are uniformly packed, it follows that the sum of the attractive forces inside the core and the interaction between (surface) chain segments and solvent can be expressed, approximately, as $f_s=g+\gamma a$. Here, g is a constant attractive term which may be set to zero and γ is the surface (hydrocarbon-water contact) free energy per unit area, often identified with the water-hydrocarbon surface tension. Thus, according to our MF theory $f=f_c+f_s=f_c+\gamma a$, implying $\partial f/\partial a=\partial f_c/\partial a+\gamma$.

From the equations derived in Sec. II, it follows that $\beta f_c=\sum_\alpha P(\alpha)\ln P(\alpha)=-\ln q-\beta\sum_k\pi_k\langle\phi_k\rangle$ and $\beta\langle\phi_k\rangle=-(\partial\ln q/\partial\pi_k)$. Hence $df_c=-\sum_k\pi_k d\langle\phi_k\rangle$, revealing that df_c is a generalized ‘‘PV’’ work, and confirming the interpretation of the π_k 's as lateral (or tangential) pressures. In Sec. II we noted that $P(\alpha)$ and thus f_c remain invariant upon adding an arbitrary constant to all the π_k 's. This also follows from the last expression for df_c : changing π_k to π_k+c yields $df_c=-\sum_k\pi_k d\langle\phi_k\rangle-c\sum_k d\langle\phi_k\rangle=-\sum_k\pi_k d\langle\phi_k\rangle$ because $\sum_k d\langle\phi_k\rangle=d\sum_k\langle\phi_k\rangle=dn\equiv 0$. Now, for a symmetric bilayer $2df_c=-\sum_k\pi_k[d\langle\phi_k\rangle+d\langle\bar{\phi}_k\rangle]=-\sum_k\pi_k dm_k$, so that

$$-\left(\frac{\partial f_c}{\partial a} \right)_v = \frac{1}{2\nu} \sum_{k=1}^{2L} \pi_k \left(\frac{\partial m_k}{\partial a} \right)_v = \frac{1}{\nu} \sum_{k=1}^L \pi_k \left(\frac{\partial m_k}{\partial a} \right)_v, \quad (9)$$

where the m_k 's are the differential volumes corresponding to the different sublayers of the hydrophobic core. The m_k 's are legitimately treated here as variables, but it should be remembered that in a planar symmetric bilayer all $m_k=m$ are equal, and $\sum_k m_k=2Lm=2\nu$ where $\nu=n\nu$ is the chain volume. In the second equality in Eq. (9) we have used the symmetry relation $\pi_k=\pi_{2L-k+1}$.

The derivative in Eq. (9) corresponds to an area change of the bilayer at constant volume, which implies a change in the membrane thickness, namely, $dD=d(\nu/a)=-(\nu/a^2)da=-(D/a)da$. In our discrete representation of the bilayer as a stack of sublayers (of constant width λ) a change in $D=L\lambda$ corresponds to a change in L , i.e., in the ‘‘removal’’ of sublayers when a increases. We could extend the formalism of Sec. II to allow for a change in λ , but this would introduce another Lagrange multiplier, representing a normal component of the conformational pressure. Instead of this awkward procedure we employ the following scheme. Since the π_k 's are defined up to an arbitrary additive constant we choose this constant so that the lowest π_k is zero. In general, we find that the lowest lateral pressure is at the bilayer midplane, implying $\pi_L=\pi_{L+1}=0$. This choice is supported by MF calculations for adsorbed monolayers¹² (where there is no normal conformational pressure) and brushes,¹³ where one finds that the lateral conformational pressure drops to zero, identically, towards the chain end regime. Furthermore, numerical calculations of $\partial f_c/\partial a=-\langle\lambda/\nu\rangle\sum_k\pi_k$ (see below) yield the same results as those obtained with $\pi_L\equiv 0$. Suppose now that we increase a while keeping D constant and ensuring that the segment density in all sublayers, except L and $L+1$, remains constant. Then for all these sublayers $(\partial m_k/\partial a)=(\partial m/\partial a)=\lambda$. The number of segments in the two central sublayers ($L, L+1$) necessarily decreases slightly, i.e., $\partial(\langle\phi_L\rangle+\langle\bar{\phi}_L\rangle)/\partial a=\partial m_L/\partial a<0$, but since $\pi_L=0$, this does not affect the value of $\partial f_c/\partial a$. Thus returning to Eq. (9), we can write

$$\left(\frac{\partial f_c}{\partial a} \right)_v = -\left(\frac{\lambda}{\nu} \right) \sum_{k=1}^L \pi_k = -\int_0^D dz \pi_c(z) \quad (10)$$

with the second equality representing the continuum limit $\lambda/L\ll 1$, ($z=k\lambda, D=L\lambda$). We shall refer to $\pi_c(z)=\pi_k/\nu$ as the conformational contribution to the tangential pressure in the bilayer.

We noted earlier that $f=f_c+\gamma a$. Thus using Eqs. (8) and (10), we can write

$$\Gamma = \int_0^D dz [p_N - \pi_c(z)] + \gamma. \quad (11)$$

This equation closely resembles the familiar expression for the surface tension, σ , between two bulk phases¹¹

$$\sigma = \int dz [p_N - p_T(z)] \quad (12)$$

with p_N denoting the normal pressure and $p_T(z)$ the tangential pressure. The integration in Eq. (12) extends from one bulk phase ($z \rightarrow -\infty$) to another ($z \rightarrow +\infty$); in both limits, $p_T(z) = p_N$. In practice only a narrow interfacial region contributes to the integral.

Comparing Eqs. (11) and (12) we can identify $\pi_c(z) - \gamma/D \equiv \Pi_T(z)$ as the tangential pressure profile in the membrane. Furthermore, recall that $\pi_c(z)$ in the MF theory accounts only for the conformational, inter-chain, pressure which we attribute to the repulsive, excluded volume, interactions between neighboring chains. Thus $-\gamma/D$ can be interpreted as the (negative) contribution to the tangential pressure, arising from the attractive parts of the inter-chain potential. In our MF theory we assume uniform segment density (i.e., the segment density is the same for all z) which explains the constant contribution of the attractive potentials to $\Pi_T(z)$. The uniform density assumption is of course an approximation. It was made to allow us to calculate the conformational chain statistics, i.e., $P(\alpha)$, which is dominated by the repulsive interactions. Clearly, however, even small density gradients may strongly affect the attractive contribution to the tangential pressure.

Lipid bilayers are generally tensionless. Namely, the repulsive (inter-tail and inter-head group) interactions exactly balance the attractive (“hydrophobic”) forces. This balance determines the equilibrium thickness D (and hence the area) of the membrane. For a tensionless membrane $\Gamma = 0$ and from Eq. (11) we find

$$\int_0^D dz \pi_c(z) = Dp_N + \gamma. \quad (13)$$

The effective hydrocarbon–water surface tension, appropriate for lipid bilayers and micelles is typically estimated as $\gamma \approx 50$ dyn/cm. Thus with $p_N \approx 1$ atm $\approx 10^8$ dyn/cm² and $D \approx 10$ Å $= 10^{-7}$ cm we find $Dp_N \ll \gamma$. In other words, the repulsive chain interactions ($\pi_c(z)$), which tend to increase the membrane area, act mainly against the surface tension γ which acts in the opposite direction.

In the MC simulations presented in the next section we calculate the tangential pressure profile using the molecular theory of Kirkwood–Buff⁹ and Harasima.¹⁰ This quantity, here denoted as $\tilde{p}_T(z)$, is given by

$$\tilde{p}_T(z) = -\frac{1}{4} \int d\mathbf{r}_{12} u'(r_{12}) \left(\frac{x_{12}^2 + y_{12}^2}{r_{12}} \right) \rho^{(2)}(r_{12}, z, z + z_{12}) \quad (14)$$

with $u'(r)$ denoting the derivative of the intermolecular potential between two particles with respect to their distance, r . x_{12}, y_{12} , and z_{12} denote the Cartesian components of \mathbf{r}_{12} and $\rho^{(2)}(r_{12}, z, z + z_{12})$ is the two point distribution function, which is proportional to the probability of finding one particle at distance z from the (mathematical) phase boundary and the other at distance $z + z_{12}$ from this boundary, at distance r_{12} from the first particle. (The interface is parallel to the xy plane.) The calculation of \tilde{p}_T from the simulation results is similar to that used in Ref. 3.

In our calculation of $\tilde{p}_T(z)$ the particles are the different chain segments, and the interactions involve all non-bonded segments belonging to either the same or different chains. We model $u(r)$ as a Lennard-Jones potential and hence $\tilde{p}_T(z)$ involves both attractive (negative) and repulsive (positive) contributions. Unlike in the MF calculations we do not expect the attractive contributions to $\tilde{p}_T(z)$ to be independent of z , because the density may vary slightly with z . In turn this variation may also affect the repulsive contributions to $\tilde{p}_T(z)$. Thus the most meaningful comparison between the MF and MC calculations should involve $\pi_c(z) + \gamma/D$ on the one (MF) hand and $\tilde{p}_T(z)$ on the other (MC) hand. However, since in both the MC and MF calculations we simply impose a given membrane thickness $2D$ rather than allowing the membrane equilibrate, we do not really know γ nor p_N . [We could assume, of course, that the membrane is balanced and infer the value of $\gamma + Dp_N$ from Eq. (13).] Accordingly, the difference between $\pi_c(z)$ and $\tilde{p}_T(z)$ involves an arbitrary, unknown, constant. There is also an uncertain, multiplicative, constant in the definition of $\pi_c(z)$, namely, the effective segment volume, ν [see Eq. (10)]. Thus in the comparisons between $\tilde{p}_T(z)$ and $\pi_c(z)$ reported in the next section we have adopted the following procedure: We have adjusted the minimum of $\pi_c(z)$ and $\tilde{p}_T(z)$ to coincide (thus eliminating γ) as well as their maximum (thus determining ν), for one particular membrane thickness D . The value of ν evaluated by this procedure was then used in all other calculations for both pure and mixed bilayers. As we shall see, the value obtained for ν is quite reasonable (comparable to that of a chain segment) and the shapes of $\pi_c(z)$ and $\tilde{p}_T(z)$ are generally very similar to each other.

V. RESULTS AND DISCUSSION

Monte Carlo simulations and mean field calculations were carried out for pure ($n=10$) and mixed ($n=10$, $m=5$) bilayers, using the chain model described in previous sections. All simulations were performed for bilayers composed of 200 chains, 100 per monolayer, with periodic boundary conditions in the xy plane. The head groups were anchored to the interfaces by a harmonic binding potential, allowing only small amplitude fluctuations (of approximately $2/3\sigma$) of the chain along the z axis. In all cases the bilayer thickness D , and hence the average area per head group a , was adjusted so as to achieve nearly uniform segment density within the hydrophobic core, and yet allow the chains to sample as many conformations as possible on the time scale of the simulations. We found that this balance depends rather sensitively on the inter-segment interaction potential. For example, using 6-12 Lennard-Jones potentials, as we did in most simulations, uniform segment density was rather easily obtained. On the other hand it was difficult to achieve uniform density (and reasonable chain dynamics) when we used a “sticky-balls” potential, (i.e., $-1/r^6$ attraction and infinite, hard core, repulsion). For the pure systems the membrane thicknesses studied ranged from $D = \nu/a \approx 5\sigma$ to $\approx 7\sigma$, corresponding to areas per head group from $a \approx 2.44\sigma^2$ to $a \approx 1.69\sigma^2$. In all cases the segment volume fraction was

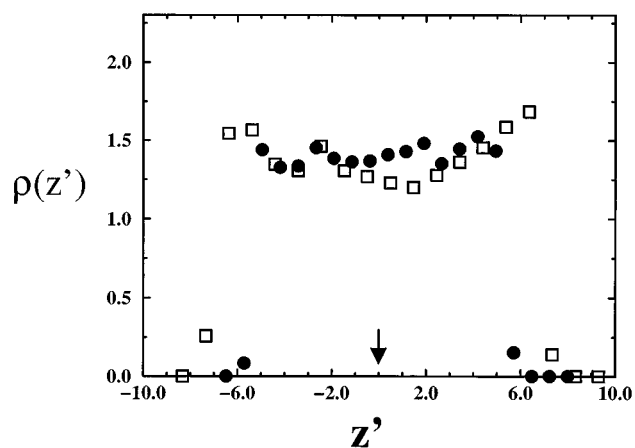


FIG. 3. Segment density along the z axis for two bilayers composed of 10 segment chains: $D \cong 4.9\sigma$ (solid circles) and $D \cong 6.4\sigma$ (squares), head groups being bound by a harmonic potential to the interface. The arrow marks the membrane midplane.

$\rho \cong 0.44$, corresponding to $\rho\sigma^3 \cong 0.84$. This value is typical of liquid-like alkane densities at ordinary temperatures. It must be noted however, that for comparison with the MF results we only require uniform segment densities. Slightly lower or higher values of ρ should yield similar results, as long as the density within the simulated bilayer is uniform. Several compositions of mixed chain systems (used to compare the lateral pressure) were also considered, again maintaining a constant ρ .

A. Segment density

As noted in Sec. III B the demand for a uniform segment density is *a priori* in the MF calculations, while it is not so in the MC simulation. It was thus a primary requirement that the uniform density condition be satisfied in the MC simulation. As can be concluded from Fig. 3, which shows the density profile in the bilayer obtained for a system with LJ interaction potentials, this assumption is valid within reasonable deviations from the mean. For a system governed by ‘‘sticky-ball’’ potentials (Fig. 6a below), it was difficult to satisfy this condition. This system was still used for reference, due to the fact that some of the chain properties compared better to the MF calculations.

B. End segment distribution

The end segment distribution along the membrane normal in a bilayer composed of $n=10$ chains is shown in Fig. 4 for two values of the membrane thickness: $D=4.9\sigma$ and 6.4σ . (The maximal value of D for 10-segment chains is 9.5σ , corresponding to a solid-like membrane of fully stretched chains, all along the membrane normal). The results in Fig. 4 show very good agreement between the MF theory and the simulations.

In both systems the end-segment distribution peaks at the membrane midplane, and reveals considerable interdigitation (monolayer crossing) of chains belonging to the two monolayers.

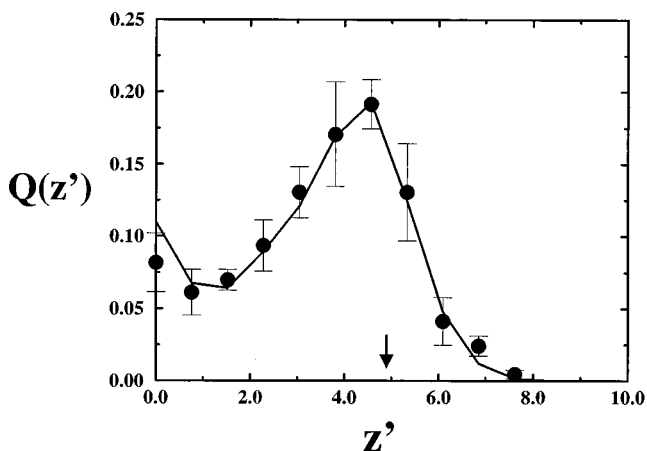
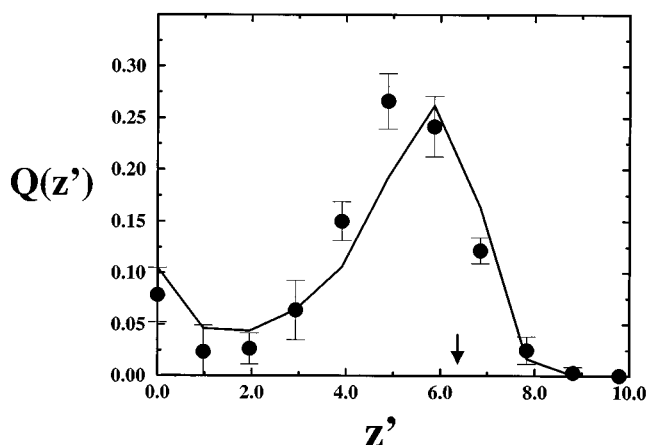


FIG. 4. End segment distribution for the same two systems mentioned in Fig. 3: $D \cong 6.4\sigma$ (top) and $D \cong 4.9\sigma$ (bottom). In each case, the MC results are marked by circles, with error bars for 5 averaging runs, and the MF calculations are marked by a solid line. The arrows mark the membrane midplane for each case.

We note that the MF/MC agreement is better for the smaller membrane thickness. This may be correlated with the fact that for this system the uniform density condition is better satisfied, Fig. 3. Indeed, as we increased D the agreement between the MC and MF results became gradually less impressive, as did the deviation of the MC density profiles from a uniform distribution. In general, it was more difficult to satisfy the uniform density condition in the simulations as we increased the membrane thickness D . This reflects the fact that as the area per head group decreases the conformational (and concomitantly the motional) freedom of the chains is reduced. In other words it takes longer and longer for the chains to equilibrate on a reasonable simulation time scale.

C. Orientational order parameters

Orientational bond order parameters calculated by the MF and MC schemes are shown in Fig. 5, for the same two cases considered in Fig. 4. Although the trends and magnitudes of the order parameter profiles are similar, the agree-

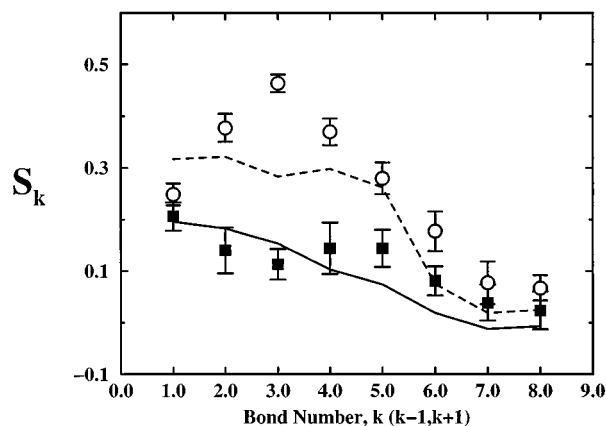


FIG. 5. Orientational order parameters for the two systems mentioned in Figs. 3 and 4: (i) $D \approx 4.9\sigma$, solid squares denoting MC results, and solid line denoting MF calculations. (ii) $D \approx 6.4\sigma$, circles denoting MC results and dashed line marking MF calculations.

ment between the MC and MF results is not as good as we found for the end segment distributions. The S_k 's derived from the MC simulations are generally higher than those obtained from the MF calculations.

We do not have a simple explanation for this discrepancy. Yet it should be noted that the orientational order parameters are very sensitive to the simulation model used. For instance, if instead of the LJ potential we use a sticky-balls interaction potential, the agreement between the MC and MF results improves considerably (Fig. 6), even though the density profile in the simulations is not exactly uniform. In fact, it was shown elsewhere, that the agreement between order parameter profiles computed by our MF scheme, for chains modeled using the rotational isomeric state scheme, compare very well with molecular dynamics simulations of similar (though not exactly the same) chains.^{1,5,6} Rotational isomeric chains are considerably stiffer than the (freely rotating) chains simulated here, hence their conformational phase space is considerably smaller than in our present model, and sampling their conformational space is simpler. In other words, it is possible that, despite the very long times of our simulation runs, the system has not reached complete equilibrium. There still remains a question as to why certain properties (like end-segment distributions) show smaller differences between the MC and MF calculations. One possible explanation is that the MC simulations have in fact reached equilibrium but there are some inherent differences between the two approaches, which are reflected only in certain properties; after all, the MF theory neglects inter-chain correlations. But then it is not obvious which quantities will be more sensitive to such correlations.

D. Lateral pressures

The results of the MF and MC calculations for the tangential pressure profiles are shown in Fig. 7 for four representative systems. Two of these, Figs. 7a and 7d, describe the results for pure bilayers composed of long ($n=10$) and short ($m=5$) chains, respectively. Figs. 7b and 7c corre-

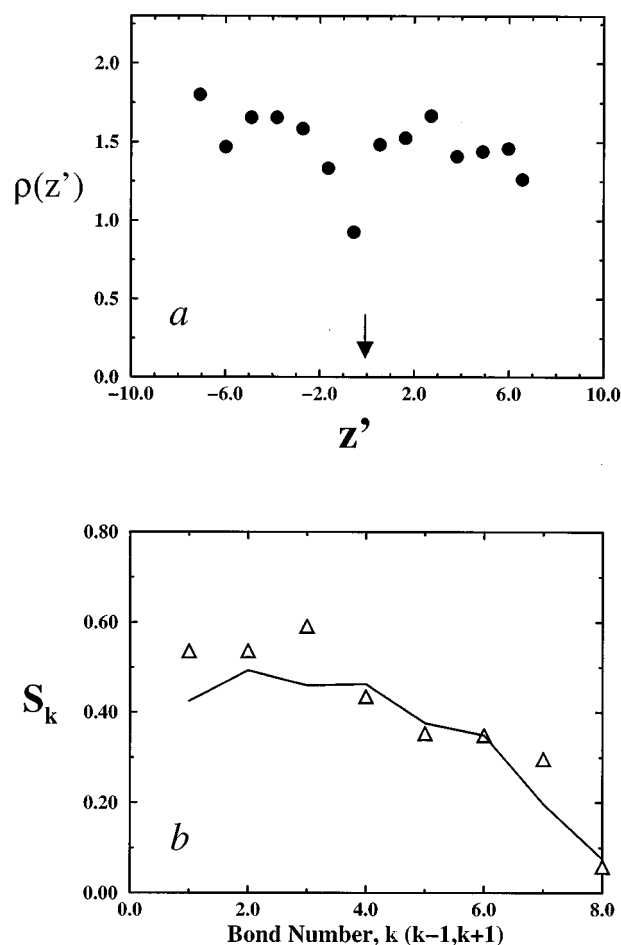


FIG. 6. Results for a system using a "sticky-balls" potential: (a) Segment density along the z axis, for a bilayer of thickness $D \approx 6.7\sigma$, composed of 10-segment chains. The chain heads are bound to the interface by a square well potential. (b) Orientational order parameters for the same system, triangles denoting MC results and solid line denoting MF calculations. The arrow marks the membrane midplane.

spond to mixed bilayers, in which the long chain mole fractions are $x=2/3$ and $1/3$, respectively. In all four systems we keep the area per head group constant ($a=2.42\sigma^2$), and ensure constant segment density (volume fraction $\rho \approx 0.44$). Accordingly, the membrane thickness varies from $D \approx 4.9\sigma$ for the long chain bilayer, to $D \approx 2.45\sigma$ for the short chain system.

As reasoned in Sec. IV we have adjusted the scale of the MF pressures to that of the MC calculations as follows. We multiply the MF lateral pressures by a constant (ν , an "effective volume per segment") to adjust the scale to that of the MC results, and then add a constant to fit the minima of the two profiles. Using a single value of $\nu \approx 1\sigma^3$, corresponding to a volume fraction $\rho = (4\pi/3)(\sigma/2)^3/\nu \approx 0.52$, we obtained good agreement between the MF and MC results for all four cases (as well as for several other cases which are not shown here). Regardless of this adjustment it should be noted that the MC and MF pressure profiles appear similar, except for some deviations near the interfacial regions (where segment crowding tends to take place in the

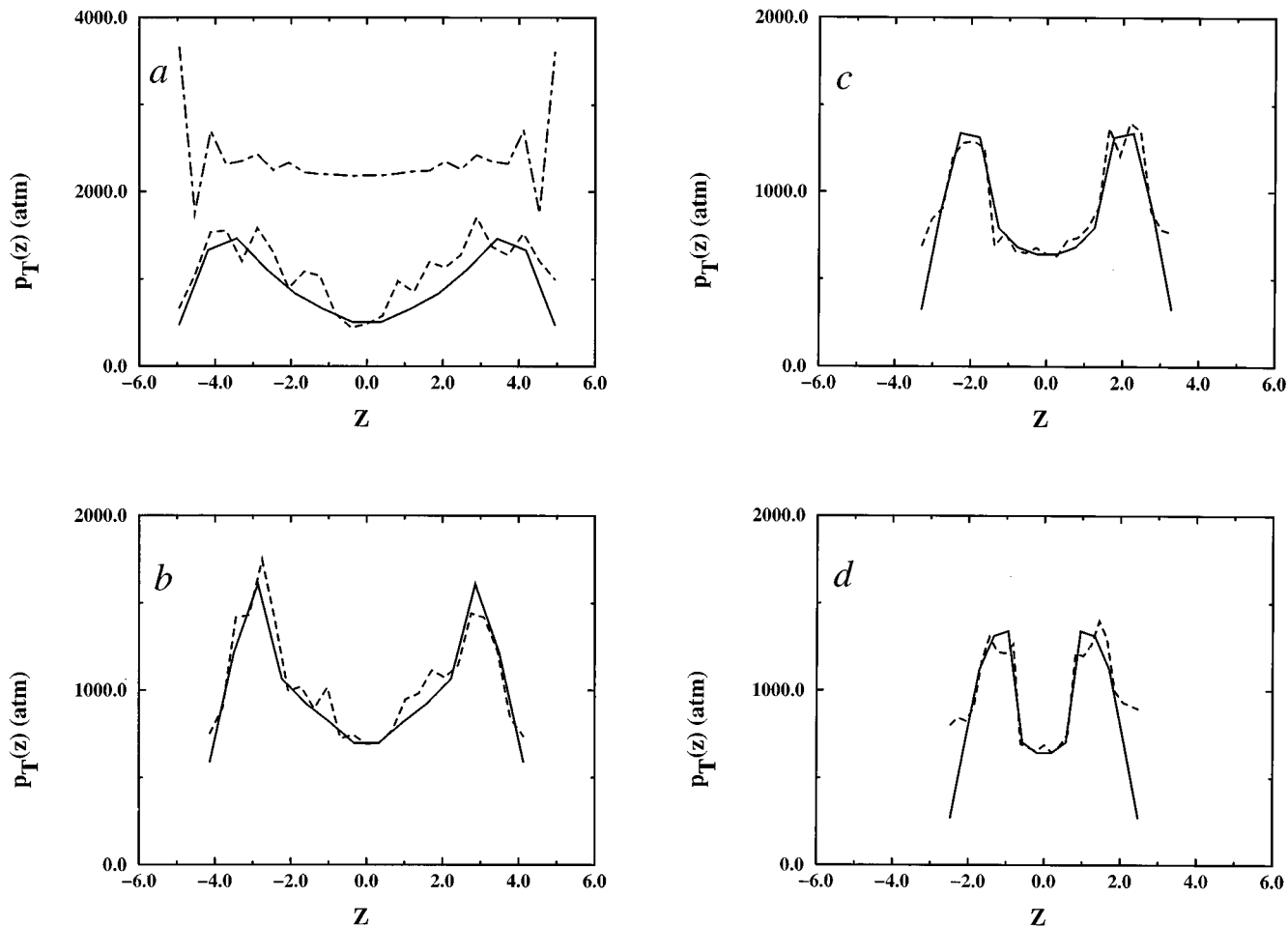


FIG. 7. Lateral pressure profiles for bilayers composed of long ($n=10$) and/or short ($m=5$) chains. (a) A pure bilayer of long chains ($D \cong 4.9\sigma$). The dashed line denoting MC results and the solid line denoting MF calculations. Also shown is the tangential pressure profile obtained by simulations of a system where all segments are disconnected (dot-dashed line). (b) Lateral and tangential pressures for a mixed bilayer. The mole fraction of long chains is $x=0.67$ ($D \cong 4.1\sigma$). (c) $x=0.33$ ($D \cong 3.3\sigma$). (d) $x=0$, i.e., a pure bilayer of short chains, ($D \cong 2.5$). As in (a) the solid and dashed lines in (b)-(d) correspond, respectively, to the MF and MC simulations.

simulations). The somewhat jagged appearance of some of the MC profiles reflects a tendency for segment layering induced by the existence of the interfacial “wall” boundaries.

Although we treated ν as an adjustable parameter, its numerical value is actually very similar to what we should have expected. Recall first, from Sec. II, that this parameter, representing the average volume per segment in the membrane, does not really enter our calculation of the MF pressure profile. It only appears, as a conversion factor, if we insist that the condition of uniform segment density (constant ϕ_k 's) also implies liquid like density. On the other hand, the actual segment volume can simply be evaluated from our MC model, namely from $\nu = V/(2Nn)$, where V is the membrane volume and $2Nn$ is the total number of segments in this volume. This gives $\nu \cong 1.2\sigma^3$. Thus the “effective” ν derived from the fitting procedure is in fact just slightly smaller than the real segment volume.

Although the difference between the two values of ν is not very significant, the smaller value of the “effective” volume, suggests that the average distance between non-bonded chain segments is somewhat smaller than that ex-

pected for a system packed at liquid like density. This implies enhancement of the (nearly) hard core repulsive interactions, in the simulated system. This trend, i.e., the dominance of the repulsive interactions is confirmed by the high (positive) values of the MC tangential pressures, as follows directly from Eq. (14).

In the MF calculations the doubly peaked pressure profile reflects, exclusively, the lateral stress profile associated with the restricted conformational freedom of the tightly packed chains in the membrane. This conformational pressure is a direct result of chain connectivity. In order to test whether the similar, double-peak, tangential pressure profile in the simulations is also associated with chain connectivity, we have performed one set of simulations for “disconnected chains.” That is, we disconnected all bonds between chain segments, thus obtaining a simple LJ fluid of the same density and boundary conditions (two interfacial walls) as the connected system. The resulting tangential pressure profile is shown in Fig. 7a. The interesting point that concerns this disconnected system is that the lateral pressure profile is nearly uniform in the bulk fluid, (becoming irregular only

near the boundary walls, due to the crowding of segments in that region).

VI. CONCLUDING REMARKS

The mean field theory described in this paper has already been applied to a variety of systems and phenomena, that either have not or cannot be studied by computer simulations. It was used, for example, to analyze the vesicle-micelle phase transition induced by the addition of surfactant molecules to lipid vesicle bilayers,⁴ a process of interest for membrane reconstitution and solubilization. Another application concerns the calculation of curvature elastic moduli of pure and mixed membranes.^{1,5} In both cases the mean field theory predicted correctly the qualitative trends, and in most cases also the quantitative behaviors, observed in experimental studies of these systems.

Since the mean field theory is much simpler to implement than large scale computer simulations, we found it important to test it by direct comparison with computer simulations for the same model system. The agreement found between the two approaches is generally very good, although some issues remain unclear. For instance, why certain conformational properties agree very well while others show some deviations. It should also be noted that we found some differences between simulations involving apparently unimportant variations of the interaction potential. Correspondingly, the agreement between the simulation and the MF approach is also (somewhat) variable. On the one hand this may be regarded as a limitation of the MF theory. On the other hand this supports its use as a “robust” tool, mainly for predicting qualitative trends and behaviors. Additional studies, involving different chain models may shed more light on such questions, and may indicate the limitations of the mean field approach or possibly, how it could be improved.

We have devoted special attention to the comparison between the mean field lateral pressures and the tangential pressures from the Monte Carlo simulation. We found good agreement between the two methods of calculation and a consistent scale relationship between the two types of pressure profiles. This finding is of particular importance since the pressures are the only molecular-thermodynamic parameters governing the probability distribution of chain conformations.

Moreover, the lateral pressures appear explicitly in the molecular expressions for the various thermodynamic properties, e.g., the stretching and bending moduli of lipid membranes.^{1,4}

ACKNOWLEDGMENTS

This work was partly supported by the US–Israel binational Science Foundation and by the Israel Science Foundation. The Fritz Haber research center where this research was performed is supported by the Minerva foundation, Munich, Germany.

¹For reviews, see (a) A. Ben-Shaul, in *Membranes: Their Structure and Conformations*, edited by R. Lipowsky and E. Sackmann, (Elsevier, Amsterdam, 1995), Chap. 7, p. 359; (b) A. Ben-Shaul and W. M. Gelbart, in *Micelles, Membranes, Microemulsions and Monolayers*, edited by W. M. Gelbart, A. Ben-Shaul, and D. Roux (Springer, New York, 1994), Chap. 1, p. 1.

²See, for example: (a) K. A. Dill, J. Naghizadeh, and J. A. Marqusee, *Annu. Rev. Phys. Chem.* **39**, 425 (1988); (b) D. W. R. Gruen, *J. Phys. Chem.* **89**, 146 (1985); (c) F. A. M. Leermakers and J. M. H. M. Scheutjens, *J. Chem. Phys.* **89**, 3264 (1989); (d) S. Marčelja, *Biochem. Biophys. Acta* **367**, 165 (1974); (e) R. S. Cantor, *J. Chem. Phys.* **103** (1995); (f) N. J. Zoeller, and D. Blankschtein, *I&EC Res.* **34**, 4150 (1995).

³T. Xiang and B. D. Anderson, *Biophys. J.* **66**, 561 (1994).

⁴I. Szleifer, D. Kramer, A. Ben-Shaul, W. M. Gelbart, and S. A. Safran, *J. Chem. Phys.* **92**, 6800 (1990).

⁵A. Ben-Shaul, I. Szleifer, and W. M. Gelbart, *J. Chem. Phys.* **83**, 3597 (1985).

⁶D. R. Fattal and A. Ben-Shaul, *Biophys. J.* **67**, 983 (1994). See also, D. R. Fattal and A. Ben-Shaul, *Physica A* **220**, 192 (1995).

⁷M. A. Carignano and I. Szleifer, *J. Chem. Phys.* **100**, 3210 (1994); M. A. Carignano and I. Szleifer, *ibid.* **102**, 8662 (1995).

⁸See, for example, S. Milner, *Science* **251**, 905 (1991).

⁹J. G. Kirkwood and F. P. Buff, *J. Chem. Phys.* **17**, 338 (1949).

¹⁰A. Harasima, *Adv. Chem. Phys.* **1**, 203 (1958).

¹¹J. S. Rowlinson and B. Widom, *Molecular Theory of Capillarity* (Clarendon, Oxford, 1982).

¹²I. Szleifer, A. Ben-Shaul, and W. M. Gelbart, *J. Phys. Chem.* **94**, 5081 (1990).

¹³I. Szleifer and M. A. Carignano, in *Advances in Chemical Physics Vol. XCIV, Polymeric Systems*, edited by I. Prigogine and S. A. Rice (Wiley, New York, 1996), p. 165.

¹⁴T. C. Clancy and S. E. Webber, *Macromolecules* **26**, 628 (1993).

¹⁵M. Lal, *Mol. Phys.* **17**, 57 (1969).

¹⁶N. Madras and D. Sokal, *J. Stat. Phys.* **50**, 109 (1988).

¹⁷B. MacDonald, N. Jan, D. L. Hunter, and M. O. Steinitz, *J. Phys. A* **18**, 2627 (1985).